AUTOMATIC DETECTION OF SUBTLE FOCAL CORTICAL DYSPLASIA USING SURFACE-BASED FEATURES ON MRI

Pierre Besson[a,c], Olivier Colliot[b], Alan Evans[c] and Andrea Bernasconi[a,c]

[a]Neuroimaging of Epilepsy Laboratory, Montreal Neurological Institute, Montreal, Canada
[b]Cognitive Neuroscience and Brain Imaging Laboratory, CNRS UPR 640-LENA, Université Pierre et Marie Curie - Paris 6, Hôpital de la Pitié-Salpêtrière, Paris, France
[c]McConnell Brain Imaging Centre, Montreal Neurological Institute, Montreal, Canada

ABSTRACT

Focal cortical dysplasia (FCD) is an important cause of pharmacoresistant epilepsy. Small FCD lesions are difficult to distinguish from non-lesional cortex and remain often overlooked on radiological MRI inspection. This paper presents a method to detect small FCD lesions on T1-MRI relying on surface-based features: cortical thickness, gradient magnitude at the white-matter / grey-matter interface, cortical signal intensity, curvature and depth of inner-cortical surface. These features best describe the visual and morphometric characteristics of small FCD, and allow differentiating it from healthy tissues. The automatic detection was performed by a neural-network bagging trained on manual labels. The method was tested on 19 patients with small FCD and identified the lesion in 89% (17/19) of cases. Cluster analysis demonstrated that the lesional cluster was the largest in 76% (13/17) of identified cases. This new approach may assist the presurgical evaluation of patients with intractable epilepsy, especially those with "MRI-negative" epilepsy.

Index Terms— Magnetic resonance imaging, Nervous system, Biomedical signal detection, Biomedical image processing, Neural network applications.

1. INTRODUCTION

Malformations of cortical development (MCD) have been increasingly recognized as an important cause of pharmacoresistant epilepsy. Focal cortical dysplasia (FCD) [1], a malformation due to abnormal neuroglial proliferation, is the most frequent MCD in patients with intractable extra-temporal epilepsy [2]. Epilepsy surgery, consisting in the removal of the FCD lesion, is an effective treatment for these patients and magnetic resonance images (MRI) plays a pivotal role in presurgical evaluation [3].

Image analysis techniques were previously developed to detect FCD automatically on MRI, relying on different types of voxel-wise analysis [4-6]. In particular, we proposed computational models of FCD characteristics [7] and a Bayesian classifier for lesion detection [4]. While these approaches successfully identified FCD in a majority of patients, most of the lesions included in these studies were detected on routine radiological evaluation. On the other hand, the detection of small FCD lesions, which are overlooked in more than 80% of cases [8], is a much more difficult task and has never been addressed.

This paper presents a new method for detecting small FCD lesions on T1-weighted MRI, relying on surface-based MR features of FCD. To increase the sensitivity of the automated method, we developed vertex-based analysis by projecting voxel-wise features onto the cortical surface.

2. METHODS

2.1. Image acquisition and preprocessing

3D MR images were acquired on a 1.5T scanner using a T1-fast field echo sequence (TR=18, TE=10, 1 acquisition average pulse sequence, flip angle=30°, matrix size=256×256, FOV=256, thickness=1mm) with an isotropic voxel size of $1mm^3$. All images underwent automated correction for intensity non-uniformity and intensity standardization [9], automatic registration into stereotaxic space [10], automatic tissue classification [11] and brain extraction [12].

2.2. FCD features extraction

To detect the lesion, five features were extracted from the MR images. These features correspond to visual characteristics – cortical thickening, a blurred transition between gray matter (GM) and white matter (WM), and hyperintensity signal within the displastic lesion [7] – or to morphological characteristics specific to small FCD – depth from the outer cortical surface and local curvature of the cortical surface [8].

2.2.1. Extraction of cortical surfaces

In each hemisphere, the inner and outer-cortical surfaces were computed using the CLASP (Constrained Laplacian Anatomical Segmentation using Proximities) algorithm [13]. The inner-cortical surface was extracted by inflating a

sphere polygon model to the boundary between GM and WM. The outer-cortical surface was obtained by expanding the inner-cortical surface to match the boundary between GM and cerebrospinal fluid (CSF). These two surfaces are formed of 81920 corresponding vertices.

2.2.2. Cortical thickness

The cortical thickness was measured using the t-link method which is the distance between corresponding vertices [14].

2.2.3. Blurring of the WM/GM interface

The blurred WM/GM interface was modeled by applying a gradient operator on the MR image. The gradient magnitude was then interpolated at each vertex of the inner cortical surface to obtain the gradient surface map.

2.2.4. Hyperintense signal

To model hyperintensity of the lesion with respect to healthy cortex, we constructed three equidistant intra-cortical surfaces by placing three uniformly spaced vertices between linked vertices of inner and outer cortical surfaces.

The intensity of the underlying MR image was then interpolated at each vertex of the intra cortical surfaces. The intensity feature was modeled by the mean intensity of the three corresponding vertices of the intra-cortical surfaces.

2.2.5. Morphometric features

We previously demonstrated that small FCD lesions were located at the bottom of a deep sulcus [8]. To include this morphometric information into our model we measured the depth and the curvature of the inner cortical surface.

The depth was defined as the shortest distance between each vertex of the WM surface and the boundary of the brain mask obtained with the brain extraction tool (BET) [12].

The curvature was calculated at each vertex using area-minimizing flows to define a deviation from the surface to a sphere [15].

2.3. Vertex-based analysis

In the normal brain, feature values vary depending on the anatomical location. To take into account these regional variations, we proposed to use a vertex-based analysis (VBA) of the features by applying vertex-wise comparison between a group of healthy controls and a given patient. VBA included the following steps (Figure 1): 1) blurring of the features using a 5 mm FWHM Gaussian surface kernel [16]; 2) registration of the surface features to a template [15]; 3) computation of the mean and standard deviation (SD) at each vertex within the group of healthy controls; 4) deviation from normal is obtained using vertex-wise z-score transform for each patient with respect to the healthy controls' mean and SD.

We computed the VBA on cortical thickness, gradient, intensity and depth maps.

Finally, six features were selected to feed the classifier: VBA on cortical thickness, gradient and intensity maps to model the visual characteristics of the lesions; curvature and depth maps, and VBA on depth map to model the morphometric properties of the small FCD.

2.4. Neural network design

For automatic FCD classification, we chose to use four layer feed forward neural networks with following number of neurons in each layer: (6–4–4–1); tan-sigmoid function was used at each neuron and the output node resulted in a number between 0 and 1 representing the probability of being lesional.

2.4.1. Learning database

Lesions were manually segmented on 3D MRI by trained raters and interpolated at each vertex of the cortical surfaces. However, since the small FCD lesions are difficult to distinguish on T1-MRI, the user made use of other image sequences when available such as T2, proton density (PD) and fluid-attenuated inversion recovery (FLAIR). The spatial extent of the lesions being difficult to define [17], the labels were considered as silver standard.

2.4.2. Neural network training

To avoid over fitting, we used cross-validation method to optimize the nets. From all patients, we obtained a database constituted of about $2.8 \cdot 10^6$ non-lesional and 1841 lesional instances in which we randomly picked 200 vertices (80 lesional, 120 non-lesional) to construct the training set and 200 different vertices (80 lesional, 120 non-lesional) for the validation set. The neural network was optimized on the training set until the error on validation set started increasing. To avoid poorly performing nets, we used a bagging approach: we created 200 nets and kept only the best 100 (i.e. having the lowest validation error). The proportion of lesional instances in the training and validation sets and the ratio of discarded nets were ad hoc choices obtained from experiments. The final output of the networks bagging was the average of the 100 nets.

2.5. Threshold of the lesional probability map

The lesional probability maps obtained from the classifier were binarized by thresholding them at the best trade-off between detection rate and amount of false positives (FP).

2.6. Cluster analysis

The cortical surfaces are constituted of triangle meshes, each vertex being surrounded by 6 neighbours. Therefore, the cluster size was defined as the number of 6-connected

vertices. Since manual labels don't provide the exact extent of FCD, vertices belonging to a cluster connected to the label were considered true positives.

3. EXPERIMENT AND RESULTS

3.1. Subjects

We studied 41 consecutive patients with FCD. The volume of the lesions ranged from 128 to 94620 mm^3 (mean ± SD = 7731 ± 14891 mm^3).

Using an entropy index based on their size and visibility on routine clinical MRI examination [8], 19 patients had a lesion defined as small and therefore were included in the study (mean age = 24.9 ± 10.9). Their mean volume was 1380 ± 808 mm^3 (range: 128 – 3093 mm3), 17/19 (89%) had been overlooked on routine clinical MRI examination. The extent of the manual labels on the cortical surface was 96 ± 66 vertices (range: 14 – 236).

We used 45 healthy controls (mean age = 27.3 ± 7.8) to construct the VBA models.

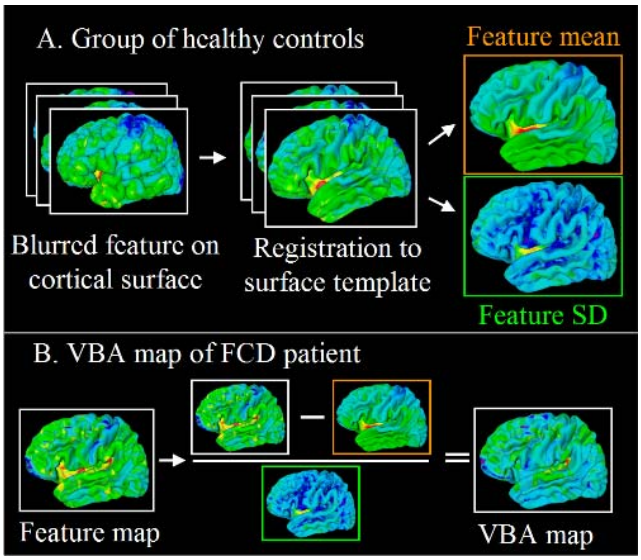

Figure 1. Generation of the VBA maps. (A) Processing steps for the healthy controls to create feature mean and SD maps. (B) The feature of a single patient is z-scored with respect to the mean and SD maps obtained at step A.

3.2. Results

We found the best trade-off between detection rate and amount of FP using a threshold value of 0.93 as illustrated in Figure 2.

Using this threshold, the classifier correctly identified the lesion in 17/19 (89%) patients. The size of the lesional cluster was 35.2 ± 45.6 vertices (range: 2 – 149). The lesional cluster was the largest in 13/17 (76%) or among the largest two in 15/17 (88%) detected cases. Summary of cluster analysis is presented in Table 1. An example of the automatic detection is shown in Figure 3.

On average, 6.1 ± 5.8 FP clusters were found in 16/19 (84%) patients and their size was 4.8 ± 6.9 vertices (range: 1 – 43). They were located in the frontal lobe (34%), central area (21%), temporal lobe (19%), insula (19%) and parieto-occipital areas (7%). Although more FP clusters were ipsilateral (55%) than contralateral (45%) to the lesion, ipsilateral FP clusters were smaller than contralateral ones (*ipsi:* 3.2 ± 4.4 (range 1 – 26); *contra:* 6.6 ± 8.8 (range 1 – 43) vertices).

Within healthy controls, the classifier created 2.5 ± 1.8 FP clusters in 25/45 (55%) individuals. The average size of the largest FP cluster was 5.5 ± 5.6 vertices (range: 1 – 26).

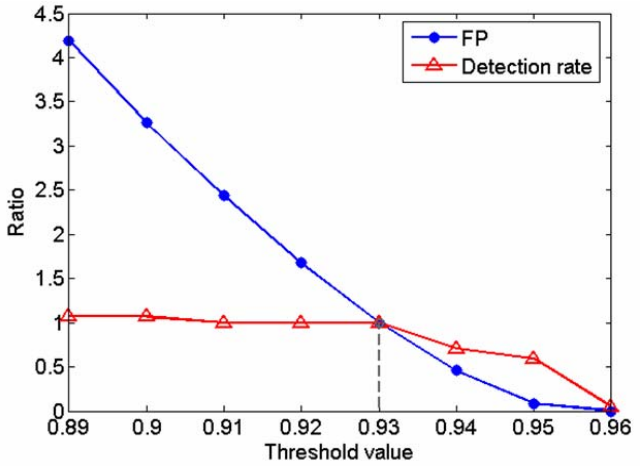

Figure 2. Detection rate and amount of FP vertices (y-axis) plotted against the lesional probability threshold. Values on y-axis are normalized with respect to that obtained at a threshold of 0.93.

Table 1. Size (in vertices) of manual labels, automatic lesional cluster and largest false positive (FP) cluster in all patients.

Patient	*Label*	*Lesion*	*FP*
01	142	149	43
02	139	130	5
03	101	93	0
04	22	85	35
05	120	45	6
06	236	44	13
07	93	29	26
08	68	22	13
09	145	17	4
10	66	15	10
11	57	12	19
12	221	8	0
13	28	7	16
14	145	6	1
15	38	4	0
16	51	2	29
17	141	2	11
18	14	0	13
19	14	0	4

4. DISCUSSION

The purpose of this study was to develop an automatic method for small FCD detection, a challenging and clinically valuable task that has not been addressed previously. We included features derived from visual observations and from morphometric characteristics specific to the small lesions. To increase the sensitivity of our model, we introduced for the first time the concept of vertex-based analysis that allowed us to compute vertex-wise deviation from a group of healthy controls. The features fed a neural networks bagging for decision making.

The efficiency of our approach is demonstrated by the fact that 17/19 (89%) small lesions were identified. In 13/17 (76%) patients the lesional cluster was the largest. However, although the size of the false positive clusters was similar in patients and healthy controls, the classifier revealed some unusually large non-lesional clusters in some patients that may be due to the presence of extra-lesional anomalies, as we previously suggested in a voxel-based study of FCD [6].

This new surface-based analysis may become a useful clinical tool to assist in the detection of subtle FCD lesions that are frequently overlooked by conventional means of analysis.

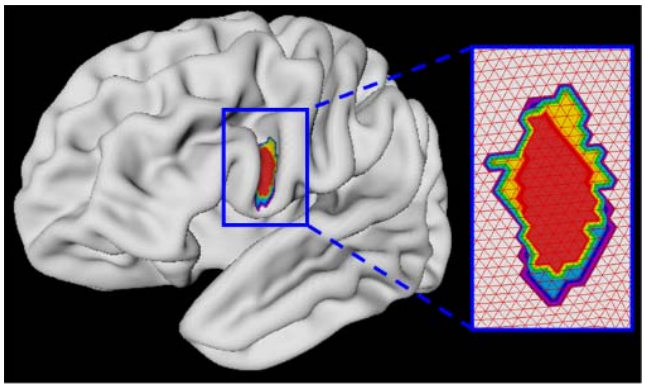

Figure 3. Result of lesion detection in patient 03 and close up on the flattened surface with overlaid vertices. *Red:* Overlap of manual label and automatic detection. *Yellow:* manual label only. *Blue:* automatic detection only. Blue vertices were considered true positives.

5. REFERENCES

[1] D. C. Taylor, M. A. Falconer, C. J. Bruton, and J. A. N. Corsellis, "Focal dysplasia of the cerebral cortex in epilepsy," *J Neurol Neurosurg Psychiatry,* vol. 34, pp. 369-387, 1971.

[2] S. M. Sisodiya, "Surgery for malformations of cortical development causing epilepsy," *Brain,* vol. 123, pp. 1075-1091, 2000.

[3] L. Tassi, N. Colombo, R. Garbelli, S. Francione, R. G. Lo, R. Mai, F. Cardinale, M. Cossu, A. Ferrario, C. Galli, M. Bramerio, A. Citterio, and R. Spreafico, "Focal cortical dysplasia: neuropathological subtypes, EEG, neuroimaging and surgical outcome," *Brain,* vol. 125, pp. 1719-1732, 8/2002.

[4] S. B. Antel, D. L. Collins, N. Bernasconi, F. Andermann, R. Shinghal, R. E. Kearney, D. L. Arnold, and A. Bernasconi, "Automated detection of focal cortical dysplasia lesions using computational models of their MRI characteristics and texture analysis," *Neuroimage,* vol. 19, pp. 1748-59, Aug 2003.

[5] M. Wilke, J. Kassubek, S. Ziyeh, A. Schulze-Bonhage, and H. J. Huppertz, "Automated detection of gray matter malformations using optimized voxel-based morphometry: a systematic approach," *Neuroimage,* vol. 20, pp. 330-43, Sep 2003.

[6] O. Colliot, N. Bernasconi, N. Khalili, S. B. Antel, V. Naessens, and A. Bernasconi, "Individual voxel-based analysis of gray matter in focal cortical dysplasia," *Neuroimage,* vol. 29, pp. 162-71, Jan 1 2006.

[7] O. Colliot, S. B. Antel, V. B. Naessens, N. Bernasconi, and A. Bernasconi, "In vivo profiling of focal cortical dysplasia on high-resolution MRI with computational models," *Epilepsia,* vol. 47, pp. 134-42, Jan 2006.

[8] P. Besson and A. Bernasconi, "Small FCD lesions are located at the bottom of a sulcus," *Epilepsia,* vol. 47, p. 16, 2006.

[9] J. G. Sled, A. P. Zijdenbos, and A. C. Evans, "A nonparametric method for automatic correction of intensity nonuniformity in MRI data," *IEEE Trans Med Imaging,* vol. 17, pp. 87-97, 1998.

[10] D. L. Collins, P. Neelin, T. M. Peters, and A. C. Evans, "Automatic 3D intersubject registration of MR volumetric data in standardized Talairach space," *J Comput Assist Tomogr,* vol. 18, pp. 192-205, 1994.

[11] A. P. Zijdenbos, R. Forghani, and A. C. Evans, "Automatic quantification of ms lesions in 3D MRI brain data sets: validation of INSECT," in *Medical Image Computing and Computer-assisted Intervention (MICCAI)*, Cambridge MA, USA, Proceedings (Lecture notes in Computer Science, 1496), 1998, pp. 439-448.

[12] S. M. Smith, "Fast robust automated brain extraction," *Hum Brain Mapp,* vol. 17, pp. 143-55, Nov 2002.

[13] J. S. Kim, V. Singh, J. K. Lee, J. Lerch, Y. Ad-Dab'bagh, D. MacDonald, J. M. Lee, S. I. Kim, and A. C. Evans, "Automated 3-D extraction and evaluation of the inner and outer cortical surfaces using a Laplacian map and partial volume effect classification," *NeuroImage,* vol. 27, pp. 210-221, 2005.

[14] D. MacDonald, N. Kabani, D. Avis, and A. C. Evans, "Automated 3-D extraction of inner and outer surfaces of cerebral cortex from MRI," *Neuroimage.,* vol. 12, pp. 340-356, 9/2000.

[15] O. Lyttelton, M. Boucher, S. Robbins, and A. Evans, "An unbiased iterative group registration template for cortical surface analysis," *NeuroImage,* vol. 34, pp. 1535-1544, 2007.

[16] J. P. Lerch and A. C. Evans, "Cortical thickness analysis examined through power analysis and a population simulation," *NeuroImage,* vol. 24, pp. 163-173, 2005.

[17] O. Colliot, T. Mansi, N. Bernasconi, V. Naessens, D. Klironomos, and A. Bernasconi, "Segmentation of focal cortical dysplasia lesions on MRI using level set evolution," *Neuroimage,* vol. 32, pp. 1621-30, Oct 1 2006.